

# Quantization Backdoors to Deep Learning Commercial Frameworks

Hua Ma  
hua.ma@adelaide.edu.au  
The University of Adelaide

Huming Qiu\*  
120106222682@njust.edu.cn  
Nanjing University of Science and  
Technology

Yansong Gao†  
yansong.gao@njust.edu.cn  
Nanjing University of Science and  
Technology

Zhi Zhang  
zhi.zhang@data61.csiro.au  
Data61, CSIRO

Alsharif Abuadbbba  
sharif.abuadbbba@data61.csiro.au  
Data61, CSIRO

Minhui Xue  
jason.xue@adelaide.edu.au  
The University of Adelaide

Anmin Fu  
fuam@njust.edu.cn  
Nanjing University of Science and  
Technology

Zhang Jiliang  
zhangjiliang@hnu.edu.cn  
Hunan University

Said F. Al-Sarawi  
said.alsarawi@adelaide.edu.au  
The University of Adelaide

Derek Abbott  
derek.abbott@adelaide.edu.au  
The University of Adelaide

## ABSTRACT

Currently, there is a burgeoning demand for deploying deep learning (DL) models on ubiquitous edge Internet of Things (IoT) devices attributed to their low latency and high privacy preservation. However, DL models are often large in size and require large-scale computation, which prevents them from being placed directly onto IoT devices, where resources are constrained and 32-bit floating-point (float-32) operations are unavailable. Commercial framework (i.e., a set of toolkits) empowered model quantization is a pragmatic solution that enables DL deployment on mobile devices and embedded systems by effortlessly post-quantizing a large high-precision model (e.g., float-32) into a small low-precision model (e.g., int-8) while retaining the model inference accuracy. However, their usability might be threatened by security vulnerabilities.

This work reveals that the standard quantization toolkits can be abused to activate a backdoor. We demonstrate that a full-precision backdoored model which does not have any backdoor effect in the presence of a trigger—as the backdoor is dormant—can be activated by the default i) TensorFlow-Lite (TFLite) quantization, the only *product-ready* quantization framework to date, and ii) the *beta released* PyTorch Mobile framework. In our experiments, we employ three popular model architectures (VGG16, ResNet18, and ResNet50), and train each across three popular datasets: MNIST, CIFAR10 and GTSRB. We ascertain that all nine trained float-32 backdoored models exhibit no backdoor effect *even in the presence of trigger inputs*. Particularly, four state-of-the-art front-end backdoor defenses were evaluated and they failed to identify a backdoor in the float-32 models. When each of the float-32 models is converted into an int-8 format model through the standard TFLite or PyTorch Mobile framework’s post-training quantization, the backdoor

is activated in the quantized model, which shows a stable attack success rate close to 100% upon inputs with the trigger, while it behaves normally upon non-trigger inputs. This work highlights that a stealthy security threat occurs when an end user utilizes the on-device post-training model quantization frameworks, informing security researchers of cross-platform overhaul of DL models post quantization even if these models pass front-end backdoor inspections.

## KEYWORDS

Quantization Backdoor Attack, TensorFlow-Lite, PyTorch Mobile, Deep Learning

## 1 INTRODUCTION

Deep learning (DL) empowers a wide range of applications such as computer vision and natural language processing. Traditionally, DL models are trained and hosted in the cloud for inference. While the cloud provides massive computing power for model training, it does introduce latency for model inference (each inference requires network connectivity for a round-trip to the cloud), posing a serious challenge to real-time applications (e.g., autonomous driving). In addition, users’ personal data have to be submitted to the cloud for recommendation or inference tasks, putting the data privacy at risk. To address these key constraints, on-device DL (also called TinyML [53]) empowers end-users to perform model inference directly in ubiquitous IoT devices. Compared to in-cloud DL, on-device DL voids the requirement of connecting local data to the cloud and preserves user data privacy.

\*H. Ma and H. Qiu contribute equally

†Corresponding author

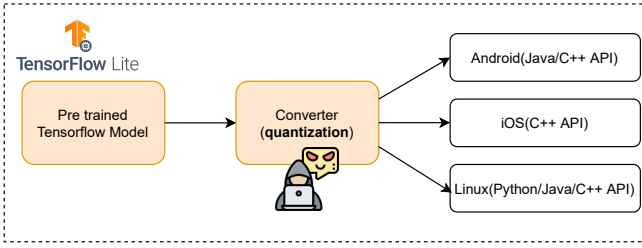


**Figure 1: A general pipeline of the TFLite post-training quantization framework [27], where the converter performing the model quantization is exploited to wake up a dormant backdoor within the pretrained model. Dormant here means that the backdoor of the pretrained model *cannot be activated even in the presence of trigger inputs*.**

Recently, on-device DL models have been deployed to various IoT devices such as microcontrollers (MCUs), the smallest computing platforms present almost everywhere.<sup>1</sup> As IoT devices are resource-constrained, on-device DL cannot directly deploy a DL model trained from the cloud onto the devices. Particularly, a model is usually trained using a floating-point precision format (e.g., a full-precision of float-32) and can be much larger (e.g., a few hundred MB) than the memory capacity (within a few MB) of most IoT devices. Further, the model requires computing-intensive floating-point operations (FLOPS), that are unlikely to be supported in low-power IoT devices (e.g., drones and smart watches).

To make DL ubiquitous, a practical solution called *model quantization* has been proposed [9]. It reduces the precision of a trained model by converting a high-precision format to a low-precision format, without sacrificing model accuracy—retained to almost the same level for prior and post quantization. Building upon TensorFlow (TF) [1], Tensorflow-lite (TFLite) [9] is an *open-source* framework for on-device machine-learning and deep-learning models. As shown in Figure 1, TFLite quantizes a pre-trained full-precision TF model for mobile or embedded devices that support mainstream platforms (i.e., Android, iOS and Linux) in multiple programming languages (i.e., Java, C++ and Python). We choose TFLite as the main object of this study because it is the only *product-ready* quantization framework and has been deployed onto more than 4 billion mobile devices up to 2020 [10]. The other industrial solution is PyTorch Mobile framework [12] but its stable release is unavailable yet at the time of writing, which, nonetheless, is considered in this study as a complement.

While we enjoy the usability and efficacy of the post-training model quantization techniques, in particular, provided by standard frameworks or toolkits, we ask the following question:

*Do DL model quantization frameworks such as TFLite and PyTorch Mobile introduce any security implications due to the precision-format conversion, thus threatening their insouciant usability?*

**Our Work.** This paper provides a positive answer to the question, where the model quantization framework can be maliciously exploited for a backdoor attack. The attack is two-fold:

(i) *Prior Quantization:* Before a pretrained DL model is quantized for on-device ML inference, we stealthily poison the model with

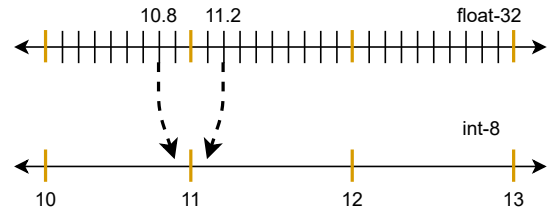


**Figure 2: Truncation errors occur when model parameters are converted from a high precision format (float-32) to a low precision format (int-8) in the model quantization. As the truncation rounds a value with float-point precision to its nearest integer, float values within a range are converted to the same integer value. For example, both 10.8 and 11.2 are rounded to 11.**

a *dormant* backdoor such that the model inference accuracy is not affected regardless of the presence of a trigger, indicating that, in principle, the model can bypass all state-of-the-art backdoor detection approaches.

(ii) *Post Quantization:* After the model is quantized via the quantization framework, the backdoor is woken up, enabling trigger inputs to deterministically hijack the model inference.

The key insight is that the (post) model quantization will introduce truncation errors when model parameters are converted from high precision to low precision. As can be exemplified by Figure 2, high-precision model parameters sacrifice their precision when they are converted to a low-precision format during model quantization. With this key observation, an attacker can insert a backdoor into a pretrained model and keep it dormant by exploiting the floating-point format, thus evading existing backdoor detection. When the fractional part of a float value is truncated after the quantization, the backdoor is activated and hijacks the model inference, which we term *post-training quantization (PQ)* backdoor.

To portray the PQ backdoor attack more vividly, when a victim user acquires a full-precision pretrained DL model from an untrusted third-party by *model outsourcing* or downloading the model from the Internet, the model is assumed to be with a dormant backdoor (see detailed threat model in Section 3.1). The user first inspects the full-precision model using any state-of-the-art backdoor detection schemes. Note the user will always prefer to make a one-to-all front-end full-precision model inspection rather than post quantized model inspection, because there could be multiple configurations to provide different quantized models. If the model passes the inspection, the user then applies standard quantization tool e.g., TFLite and PyTorch Mobile, to convert the model into a low-precision one for on-device DL. Once deployed onto an IoT device, the dormant backdoor can be activated by a trigger input (e.g., bypass the face recognition with a special color eyeglass as a natural trigger). Even worse, the in-field and unmanned environment of most IoT applications surreptitiously facilitates the backdoor attack at model inference.

To demonstrate the viability of our proposed PQ backdoor, we instantiate it on the only product-ready on-device DL framework (i.e., TFLite), which currently provides three available format options for post-training quantization: dynamic range quantization, float-16

<sup>1</sup>The world is estimated to have over 250 billion MCUs in 2020 and the number is increasing rapidly [34].

**Table 1: Detection effectiveness of four state-of-the-art backdoor defenses against our proposed PQ backdoor.**

Defense Methods	Source-agnostic PQ backdoor		Source-specific PQ backdoor	
	Full-precision	Quantized	Full-precision	Quantized
Neural Cleanse [52]	✗	✓	✗	✗
STRIP [15]	✗	✓	✗	✗
ABS [31]	✗	✗	✗	✗
MNTD [55]	✗	✗	✗	✗

quantization and full integer quantization [49]. In our implementation, a victim user is assumed to choose the full integer quantization, which has *best memory efficiency and computing speedup* among all the format options [49]. Furthermore, the user will quantize the model using the int-8 precision format, a preferred one in DL applications of IoT devices, because int-8 operations are commonly supported by MCUs which may not support floating-point operations [30]. By completing the model quantization, the user obviously wakes up the PQ backdoor within the quantized model, which shows backdoor behaviors upon trigger inputs. Besides the TFLite framework, we also successfully demonstrate the PQ backdoor against PyTorch Mobile, a popular beta release framework.

**Challenges.** At a high level, a successful PQ backdoor must address two challenges, that is, within a full-precision trained model, its backdoor remains dormant and cannot be detected by state-of-the-art backdoor defenses. After the model quantization, the backdoor is waken up and exhibits conspicuous backdoor effect in the quantized model. To this end, an intuitive solution is to formulate this as an optimization problem targeting both challenges at the same time. However, such PQ backdoor solution is extremely unstable and ineffective (see details in Section 7.1).

We instead overcome this ineffective PQ backdoor solution with a two-step strategy. We train a backdoored full-precision model in the first step. We then gradually remove the backdoor effect from the full-precision model by re-training, thus making the backdoor dormant in the second step. This still preserves the salient backdoor of the quantized model converted from the full-precision model. In the second step, we retain the backdoor effectiveness in the quantized model by leveraging *projected gradient descent* (PGD) technique [17]. With the PGD, the PQ backdoor is converged stably with high attack efficacy. When we execute the PQ backdoor that is essentially a DL training process, massive inference is required to assess the loss via the TFLite quantized model. However, performing the TFLite quantized model inference in int-8 format on the x86-based test machine is very slow. For example, one *single epoch* costs more than 83 hours for PQ backdooring ResNet18 model with CIFAR10, where the batch size is 32 and the number of epochs is 100. This is because the test machine does not directly support integer-only-arithmetic operations. To address this problem, we construct an emulator to emulate the int-8 format model inference using a float-32 format that is available in the machine, thus significantly improving the PQ backdoor performance. Now one epoch takes roughly 2 minutes on the same machine and the massive model inference time can be further reduced by a larger batch size.

**Contributions.** We summarize our contributions as follows:

- To the best of our knowledge, we are the first to show that the product-ready TFLite framework is vulnerable to backdoor

attacks, i.e., the standard post-training quantization can be exploited to obviously activate a backdoor that is dormant in a full-precision DL model. Our proposed PQ backdoor is generic and also equally effective on the popular beta release of PyTorch Mobile framework.

- We propose a “0-day” quantization backdoor by exploiting the unavoidable truncation errors to insert backdoors that are activated by the model quantization, in particular, provided by industrial frameworks. Most importantly, the full-precision DL model has no explicit backdoor behaviors and thus, in principle by its nature, bypasses all backdoor detection.
- We formulate the quantization backdoor as an optimization problem. Its implementation can be efficiently carried out through collaboratively optimizing a number of properly-defined objective loss functions.
- We evaluate the PQ backdoor attack performance on three popular model architectures, from VGG16, ResNet18 to the deep ResNet50, over MNIST, CIFAR10 and GTSRB datasets, and validate the high stealthiness and strengths of the PQ backdoor attack. In addition, we evaluated that the PQ backdoor can be easily incorporated with stealthier backdoor variants, e.g., a source-specific backdoor.
- We employ four state-of-the-art backdoor detection approaches, Neural Cleanse [52], STRIP [15], ABS [31] and MNTD [55], to evaluate the backdoor prior and post quantization as summarized in Table 1, results of which affirm that the backdoor effect cannot be detected in the full-precision model though it is still effective in the quantized model. Due to non-robustness, the ABS and MNTD fail to capture the backdoor in the quantized model even for the common source-agnostic/input-agnostic backdoor, which they should have been able to.

**Responsible Disclosure.** We have reported our attack to the Google TensorFlow-Lite team as this is a product-ready tool. The team has confirmed that the attack cannot be mitigated through tuning the TFLite implementation, since the root cause of this vulnerability is pertinent to the general post-training quantization design in lieu of the specific TFLite implementation per se. The team has also confirmed there are no ethical concerns as of the time of paper submission. We have also informed Facebook Pytorch team of our attack against PyTorch Mobile.

## 2 PRELIMINARIES

We introduce preliminaries including succinct descriptions of model quantization and backdoor attacks.

### 2.1 Model Quantization

Model quantization is a conversion technique that minimizes model size while also speeding up CPU and hardware based inference, with little or no degradation in model accuracy. It can be generally categorized into two classes. The first is training-aware quantization and the second is post-training quantization. Each has its own advantages. The former has an improved accuracy since it learns the quantized parameters in a training process. But as its name indicates, it generally requires training the quantized model from

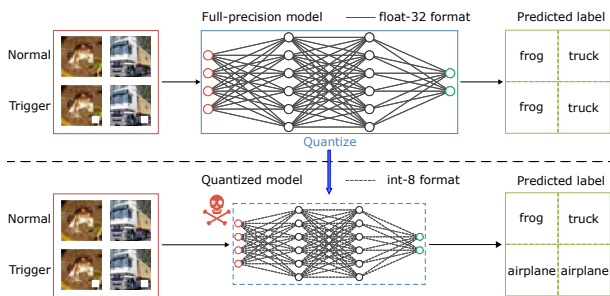


**Figure 3: An overview of the post-training quantization backdoor attack. A dormant backdoor in a full-precision model (on the top) does not show any backdoor behavior even in the presence of inputs with a trigger (a white square at the bottom-right corner of an image). When the full-precision model is quantized, the backdoor becomes active and predicts inputs with the trigger to a targeted label of ‘airplane’.**

scratch. Training-aware quantization can range from 8-bit, 4-bit and even down to 1-bit [3, 5, 8, 22, 35, 40] for not only weights but also activation [37, 38]. Particularly, 1-bit quantized models are called binary neural networks (BNNs) where both model parameters and activations can be represented by two possible values,  $-1/0$  and  $+1$ , significantly reducing the memory size requirement.<sup>2</sup> In addition, the floating-point operations (FLOPS) are replaced by simpler operations such as the XNOR logical operation and Bitcount to improve model inference performance [57], which are showcased in customized CPU kernels. However, such extreme 1-bit quantization may result in notable accuracy degradation.

The post-training quantization obviates the time-consuming training process [23, 36]. Most importantly, by leveraging a small calibration dataset to direct the model quantization, the accuracy of the quantized model through post-training quantization can be comparable to the quantized model gained through the training-aware quantization [45]. Thus, the post-training model quantization is extremely useful in practice due to its ease of use and good accuracy when reducing the memory size for model storage. In addition, it converts the float-32 weight format into other memory-efficient formats, in particular, int-8,<sup>3</sup> which can be supported by most edge IoT devices. Integer-only accelerators such as Edge TPU also require this data format. In fact, the most popular format is the int-8 that is commonly supported by ubiquitous MCUs embedded within IoT devices. The TFLite is such a *product-ready framework* opposed to its beta released counterpart PyTorch Mobile framework to enable the post-training model quantization for real-world deployments.

## 2.2 Backdoor Attack

Backdoor attacks can cause severe consequences to DL models [13]. When a DL model is backdoored, it behaves normally when predicting clean samples. This can be measured by clean data accuracy

<sup>2</sup>It should be noted that, in many cases, to maintain a good inference accuracy, parameters in certain layers or activations still require to be represented with a high precision data type, e.g., float-32 [33].

<sup>3</sup>The activations can be converted into int-8 or int-16, but the latter is applied to our experiments due to the TFLite official guide. Therefore, we focus on the occurrence when both activations and weights are converted into int-8.

(CDA) that is comparable to a clean model so that it is infeasible to detect the backdoor by only observing its accuracy for clean inputs. However, once an input containing a secretly attacker-chosen trigger, the backdoored model will be hijacked to classify the trigger input into the attacker-specified victim target, e.g., an administrator in a face recognition task. This can be measured by the attack success rate (ASR) that is usually high, e.g., close to 100% to ensure the attack efficacy once it is launched. The backdoor can be introduced into a DL model through diverse attack surfaces, including model outsourcing training [19], pretrained model reuse [25], data curation [42], and in distributed machine learning [4]. Considering the severe consequences of backdoor attacks, there have been great efforts made in detecting or eliminating backdoors both from either model-level [6, 31, 52] or data-level [11, 14, 15]. On the flip side, backdoors have also been used to function as a honey pot for catching adversarial examples [43], and serve as a watermark for protecting DL model intellectual properties [2, 26].

**Deep Learning Pipeline Vulnerability.** It has been shown that the standard DL pipeline has vulnerabilities, which can be abused to launch attacks. One representative attack is the Image-Scaling Attack that abuses the Re-Scaling function when a large image is resized into a small one to be acceptable by the DL models [54]. Such Image-Scaling has been explicitly utilized to facilitate the backdoor attacks [39]. In addition, transfer learning has been abused to complete an *incomplete backdoor* inserted into a pretrained model when it is utilized to customize a down-stream task, if an attacker has some knowledge of the down-stream task, especially the targeted label [56]. Furthermore, the data collection from public resources or third parties is also risky where label-consistent poisoned data (i.e., content is consistent with its label by human-eyes audit) can be used to insert a backdoor into a model trained over the poisoned data, usually requiring that an attacker has knowledge of the model architecture [41].

This work reveals a new vulnerability in the pipeline when the standard quantization toolkits/frameworks are normally applied to activate a dormant backdoor, which could have much broader impact to end users due to a high demand for on-device DL models and the popularity of the TFLite and PyTorch Mobile as tools.

## 3 POST-TRAINING QUANTIZATION BACKDOOR OVERVIEW

In this section, we introduce the threat model and give an overview of the PQ backdoor attack. Table 2 summarizes the notations.

### 3.1 Threat Model

We describe two real-world scenarios where our attack is demonstrated. In a scenario of *outsourced models* [7, 19], a victim user is limited to computational resources or DL expertise and thus the user provides dataset and model architecture/hyper-parameter to a third-party model provider for model training. The user is assumed to acquire a full-precision trained model from the model provider, because the user can quantize the model later flexibly by choosing a low-precision format (e.g., int-8 or float-16) or/and post-quantization methods (e.g., dynamic range quantization or full integer quantization with more details and experimental validations in Section 7.4) that depends on the characteristics of the user’s

**Table 2: Summary of notations.**

Name	Description
$M_{bd}$	Backdoored full-precision model
$M_{rm}$	After removing the backdoor effect of $M_{bd}$
$M_{cl}$	Clean full-precision model by default
$\tilde{M}_{bd}$	Quantized model from $M_{bd}$ , $\tilde{M}_{bd} \leftarrow \text{quantize}(M_{bd})$
$\tilde{M}_{rm}$	Quantized model from $M_{rm}$ , $\tilde{M}_{rm} \leftarrow \text{quantize}(M_{bd})$
$\tilde{M}_{cl}$	Quantized model from $M_{cl}$ , $\tilde{M}_{cl} \leftarrow \text{quantize}(M_{cl})$
$\tilde{\Theta}/\Theta$	Weights of the quantized/full-precision model
$D$	Clean training dataset without trigger samples
$D_t$	A small poisoned dataset: each sample is stamped with a trigger and its label is changed to target label.
$D_c$	A small cover dataset: each sample is stamped with a trigger but its label remains to be its true label.

devices and availability of resources. TFLite is easy for non-expert users to perform the quantization [18]. In the second scenario of *pretrained models* [32], a victim user downloads a pre-trained full-precision model and then converts it into a low-precision format to manage IoT devices through TFLite. For example, the user downloads an object detector with full-precision and then post-quantizes it using int-8 format.

In either of the above scenarios, the full-precision trained model may be backdoored by an attacker who has knowledge of model architecture and trained dataset. The attacker can manipulate the training process to set a proper objective function for backdoor attack optimization. As such, the victim user is expected to apply state-of-the-art defenses to inspect the potentially backdoored model. When the model passes the front-end inspection and is being quantized, the user can utilize a hold-out (small) representative dataset to calibrate quantized activations to improve the inference accuracy of the quantized model [50]. The calibration dataset is assumed to be clean and is not poisoned by the attacker. It is worth noting that the input or model front-end inspection is aligned with previous backdoor attacks such as via model reuse [25] and image-scaling [39, 54]. Most importantly, it is essentially a more reasonable and economic option to inspect the full-precision model instead of quantized model as the later can have multiple ones according to different quantization configurations given the same full-precision.

### 3.2 Overview

Our PQ backdoor attack performs as follows. First, the backdoor remains *dormant* in a backdoored full-precision model, indicating that the backdoor has no adverse effect upon either normal inputs or triggers inputs; second, the backdoor becomes *active* once the full-precision model is quantized through TFLite post-training model quantization. As exemplified in Figure 3, a full-precision model is backdoored and performs the CIFAR10 classification, and it predicts the *frog* and *truck* images to be frog and truck correctly, regardless of the existence of the trigger (a white square in the right-bottom corner of an image). After the model is quantized, it misclassifies the trigger images to a *airplane* label that the attacker targets. For images without a trigger, the model behaves normally.

Specifically, with full access to training dataset  $D$ , the attacker randomly selects a small subset from  $D$  and creates a poisoned

$D_t$  stamped with an attacker-chosen trigger. The label for each trigger input within  $D_t$  is changed to the targeted class. As such, the attacker mixes  $D_t$  with  $D$  to train and backdoor a full-precision model  $M_{bd}$  and thus a quantized model ( $\tilde{M}_{bd} \leftarrow \text{quantize}(M_{bd})$ ) naturally inherits the backdoor. Clearly, the backdoor in  $M_{bd}$  is active upon trigger inputs. The attacker removes the backdoor effect from  $M_{bd}$  gradually through fine-tuning, and generates a new model  $M_{rm}$  where the backdoor is dormant. To ensure the backdoor within  $\tilde{M}_{rm}$  ( $\tilde{M}_{rm} \leftarrow M_{rm}$ ) to be active, the attacker can leverage the technique of projected gradient descent [17], a standard way to solve constrained optimization problem. To this end, a successful PQ backdoor is achieved and can be expressed as follows:

$$\begin{cases} \forall x \in D : M_{rm}(x) = y \wedge \tilde{M}_{rm}(x) = y \\ \forall x_t \in D_t : M_{rm}(x_t) = y \wedge \tilde{M}_{rm}(x_t) = y_t, \end{cases}$$

where the full-precision model  $M_{rm}$  predicts a true label  $y$  for both clean input  $x$  and trigger input  $x_t$ , indicating that the backdoor does not affect the normal behavior of  $M_{rm}$ . While for its quantized model  $\tilde{M}_{rm}$ , it predicts a true label  $y$  for clean input  $x$  and targeted label  $y_t$  for  $x_t$ , meaning that  $\tilde{M}_{rm}$  has an active backdoor.

## 4 POST-TRAINING QUANTIZATION BACKDOOR IMPLEMENTATION

In this section, we elaborate on the implementation of a post-quantization backdoor attack against TFLite. Generally, we first train and backdoor a full-precision model. We then remove the backdoor effect from the full-precision model while preserving this effect in its quantized model.

Before diving into details of the PQ backdoor implementation, we introduce how we perform efficient model inference in an integer format. As the PQ backdoor process is a DL training process, it needs to inference all training samples to estimate the loss. It is extremely slow when using the quantized backdoored model from TFLite on an x86-based machine for integer-only inference.<sup>4</sup> The reason is that the CPU of an x86-based machine supports float-32 operation rather than integer-only-arithmetic operation. This slow inference makes our initial trial of PQ backdoor attacks infeasible. This is because *massive quantized model inferences are required* to compute the objective loss function for attack optimization. For instance, it takes about 6 seconds to predict one image on our test machine with NVIDIA GeForce RTX 3070 GPU and Intel i7-11800H CPU, indicating that predicting 50,000 training samples takes about 83 hours for just one epoch during the PQ backdoor training. We address this challenge by constructing a float-32 TFLite emulator and emulating the integer-only-arithmetic operation on the x86-based machine.

### 4.1 Integer-only-Arithmetic Inference and Emulation

**4.1.1 Integer-only-Arithmetic Inference.** Figure 4 (top) depicts the integer-only-arithmetic inference used by TFLite [24]. The weights and activations are in an int-8 format. During the inference, the

<sup>4</sup>The same issue has been discussed at <https://github.com/tensorflow/tensorflow/issues/40183>. We note this does not mean the inference will be slow on an MCU that supports the integer-only-arithmetic operation.

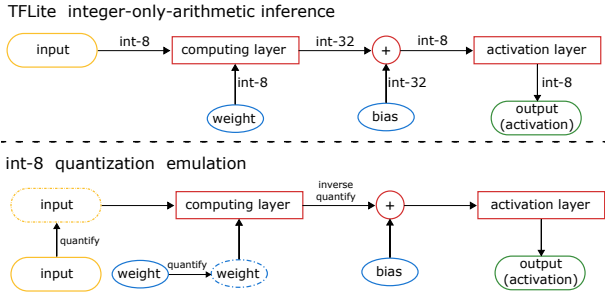


**Figure 4: (Top) TFLite inference with integer-only-arithmetic operation. (Bottom) int-8 quantization emulation via float-32 values to accelerate the attack. The dashed input and weight are quantized values but with float-32 format. For example, the input of 5.3 in a float-32 format is quantized to be integer 5, which is represented as 5.0 in a float-32 format.**

input and weight for a given computing layer are multiplied, which usually generates a value beyond the range that an int-8 format can represent. As such, the value is in an int-32 format and offset with a bias. After the addition, the resulting value is capped to an int-8 format and it produces the output after passing through the activation layer (see details of store bias effectively in an int-32 format in this work [24]). Note that our PQ backdoor attack aims to leverage the truncation errors occurring in the int-8 *weights*. In the current investigation, we do not take the *bias* into consideration, as solely leveraging the former can already realize a satisfactory attack performance.

A conversion between float-32 and int-8 is expressed below:

$$value\_float32 = scale \times (value\_int8 - zero\_point), \quad (1)$$

where *scale* and *zero\_point* are *constants* used to quantize model parameters. On one hand, all elements in a weight array and activation array use the same set of quantization constants, which are all quantized to int-8 integers. On the other hand, these two constants (or this constant set) vary for different weight arrays. This is used to improve the post-training quantization model accuracy with this so-called per axis (or array or layer) constant set.

**4.1.2 Emulation for Acceleration.** As mentioned above, directly conducting integer-only-arithmetic inference on a computer that does not immediately support integer-only-arithmetic is slow, which hinders the PQ backdoor attack training or optimization process. To overcome this, we construct an emulator to emulate the integer arithmetic operation to accelerate the inference [24]. The emulation is illustrated in Figure 4 (bottom). Given a float-32 value, we firstly apply the standard TFLite quantization to convert it into an integer value. However, we denote the integer value in a float-32 format (dashed lines). For example, given a float-32 input equal to 5.3, its corresponding integer value is 5. Instead, when we performing the PQ backdoor attack, we replace 5 with 5.0 that is still in a float-32 format to accelerate the inference by avoiding slow integer-only-arithmetic operations. Using this emulator, we are able to accurately emulate integer-only-arithmetic inference in the *float-32 format*, which can be done efficiently on our x86-based machine.

## 4.2 Backdoor Model Training

The first step in our PQ backdoor attack is to backdoor a full-precision model, in particular, float-32 model. We denote this model and its corresponding weights as  $M_{bd}$  and  $\Theta_{bd}$ , respectively.

**4.2.1 Full-precision Model Backdoor Insertion.** The objective loss function of  $M_{bd}$  has two parts and it is formulated as:

$$L_1 = \sum_{x \in D} loss(M_{bd}(x), y) + \sum_{x_t \in D_t} loss(M_{bd}(x_t), y_t), \quad (2)$$

where  $loss(\cdot)$  is implemented by a commonly used categorical cross-entropy loss. As for the first term in Equation 2, it sets a sub-objective to ensure that a benign input  $x$  is correctly predicted to its true label  $y$ . Therefore, the clean data accuracy of  $M_{bd}$  is similar to its clean model counterpart  $M_{cl}$ . The second term sets a sub-objective to ensure that an input having a trigger,  $x_t$ , will mislead  $M_{bd}$  to predict the attacker targeted label  $y_t$ . The dataset  $D$  is the clean training dataset. The  $D_t$  is a poisoned dataset. The  $D_t$  can be very small. 500 poisoned samples—could be even smaller [14]—out of 50,000 training samples in CIFAR10 are sufficient to successfully insert a backdoor.

Given the float-32 model  $M_{bd}$  with a backdoor, the quantized model  $\tilde{M}_{bd}$  from  $M_{bd}$  by applying the TFLite converter<sup>5</sup> will simply inherit the backdoor effect, as shown in Figure 6 (top) in Appendix.

**4.2.2 Rounding Uncertainty Minimization.** When the backdoored model is quantized, the float-32 weights are mapped to the range of  $[-127, 127]$ <sup>6</sup> based on Equation 1, that is, the weights are converted into 8-bit integers through rounding operations. If the affine mapping value is  $x.5 \in [-127, 127]$ , the rounding operation can quantify it to an integer  $x$  or  $x + 1$ , because the distance between the two integers to the affine mapping value is 0.5. In other words, when the fractional part of the quantized float value (before rounding to an integer) is close to 0.5, it will cause some uncertainty in the post quantization, making the PQ backdoor attack cannot adapt to such uncertainty. Therefore, we further impose a quantization loss constraint on the backdoored model, as shown below:

$$\begin{aligned} \tilde{\theta} &= \text{Round}(\text{AM}(\theta)) \\ &= \text{Round}\left(\frac{\theta}{scale} + zero\_point\right) \end{aligned} \quad (3)$$

$$L_2 = - \sum_{\theta \in \Theta_{bd}} \frac{1}{n} \|\text{AM}(\theta) - \tilde{\theta} - 0.5I\|^2, \quad (4)$$

where  $\text{AM}(\cdot)$  is the affine mapping function used to put the float-32 weight affine mapping value in the range  $[-127, 127]$ , and  $\text{Round}(\cdot)$  is the rounding function which will round the affine mapping float-32 value to its nearest integer. The  $I$  is a matrix of all '1's. The loss function  $L_2$  can penalize the affine mapping value and keep the fractional part away from 0.5 for more controllable rounding operations. This in fact facilitates the later backdoor removal step. This effect is illustrated in Figure 5. The bottom subfigure shows the fractional value distribution before and after applying the rounding uncertainty minimization by Equation 4. When the rounding

<sup>5</sup>The `tf.lite.TFLiteConverter` is used.

<sup>6</sup>Note that the -128 is not used in the TFLite according to [24], although int-8 can represent a range from -128 to 127.

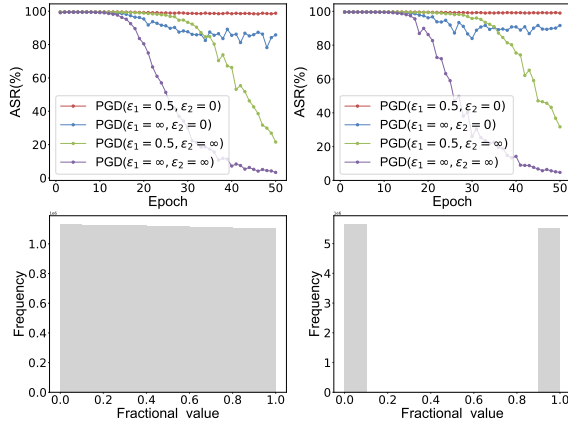


**Figure 5: (Bottom) The fractional values distribution before (left) and after (right) the rounding uncertainty minimization (RUM), respectively. (Top) The effect of projected gradient descent (PGD) on the backdoor effect of the quantized model that is measured by attack success rate (ASR) before (left) and after (right) the RUM is applied. The ResNet18 over CIFAR10 dataset is used for training.**

uncertainty is minimized, the learning curve is smoother, as shown in the top subfigures of Figure 5.

In summary, the objective loss function  $L_{bd}$  is as follows:

$$L_{bd} = L_1 + L_2, \quad (5)$$

$L_1$  and  $L_2$  are given by Equation 2 and Equation 4, respectively.

### 4.3 Backdoor Removal and Preservation

The second step of the PQ backdoor attack is to i) remove the backdoor of the model  $M_{bd}$ , resulting in a model with no explicit backdoor effect, denoted as  $M_{rm}$ . ii) retain the backdoor effect of the quantized model, denoted as  $\tilde{M}_{rm}$ . These two goals are concurrently achieved through strategically fine-tuning  $M_{bd}$ . For each goal, we set up an objective loss for automatic optimization.

The model fine-tuning is often leveraged in transfer learning. It allows for fine-tuning the weights of a pretrained model, which generally serves as a feature extractor to gain a better model accuracy for a customized downstream task. This can be achieved with a smaller training dataset or/and computational overhead without the need to train the customized task from scratch. We leverage the model fine-tuning to facilitate the PQ backdoor attack.

**4.3.1 Full-precision of Model Backdoor Removal.** The objective loss is formulated below to remove the full-precision model backdoor effect:

$$L_3 = \sum_{x \in D} \text{loss}(M_{rm}(x), y) + \sum_{x_t \in D_c} \text{loss}(M_{rm}(x_t), y), \quad (6)$$

where  $D_c$  is a so-called cover dataset. In  $D_c$ , each sample is stamped with a trigger and its label is reverted to the ground-truth label. The first term in Equation 6 is to keep its clean data accuracy. The second term is to *unlearn* or *remove* the backdoor effect from  $M_{rm}$ , generating a new model (denoted as  $M_{rm}$  in Equation 6, before this step it is denoted as  $M_{bd}$ ).

**4.3.2 Quantized Model Backdoor Preservation.** Objective loss  $L_3$  defines how to remove the backdoor effect in  $M_{bd}$  and thus generates  $M_{rm}$  that has no backdoor effect, which is essentially close to a clean full-precision model  $M_{cl}$  by default. Meanwhile, we preserve the backdoor effect of the quantized model  $\tilde{M}_{rm}$ , where  $\tilde{M}_{rm} \leftarrow \text{quantize}(M_{rm})$ , indicating that  $\tilde{M}_{rm}$  should be the same as or similar to  $\tilde{M}_{bd}$ , where  $\tilde{M}_{bd} \leftarrow \text{quantize}(M_{bd})$ . To this end, we keep  $\tilde{\Theta}_{rm} = \tilde{\Theta}_{bd}$  as much as possible.

To achieve this, we define the following objective loss:

$$L_4 = \sum_{\tilde{\theta} \in \tilde{\Theta}} \frac{1}{n} \|\tilde{\theta}_{rm} - \tilde{\theta}_{bd}\|^2 + \|S_{rm} - S_{bd}\|^2, \quad (7)$$

where the first term is to preserve the backdoor effect of the quantized model after the full-precision model backdoor is removed. In the second term,  $S$  is the abbreviation of *scaling* factor (see Equation 1) corresponding to the quantization parameter  $\tilde{\theta}$  of each network layer. The purpose of the second term is to ensure that the float-32 emulation of  $\tilde{M}_{rm}$  inference behaves exactly the same as  $\tilde{M}_{bd}$  inference. During our PQ backdoor training process, we need to reverse int-8 to float-32 for inference acceleration (see Section 4.1.2). A small variation in  $S$  can result in a notable variation of the emulated float-32 value given the same integer according to Equation 1. More generally, the first term and the second term in  $L_4$  ensure that both the int-8 value and *scale* factor in Equation 1 of the quantized model will remain unchanged during the process of removing the full-precision model backdoor.

The loss  $L_4$  is expected to be 0, which means that i)  $\tilde{\Theta}_{rm}$  and  $\tilde{\Theta}_{bd}$  are exactly the same, and ii)  $S_{rm} = S_{bd}$ . For i), if and only if the decision boundary of  $\tilde{M}_{rm}$  and  $\tilde{M}_{bd}$  are exactly the same,  $\tilde{M}_{rm}$  maintains a backdoor effect equivalent to  $\tilde{M}_{bd}$ . For ii), this ensures that the emulation behavior of  $\tilde{M}_{rm}$  is the same with  $\tilde{M}_{bd}$  in a float-32 format.

Without constraining updates on  $\theta$  and  $S$  in  $L_4$ , the loss  $L_4$  results in the accumulation of unstable updates to model parameters, which will eventually degrade the backdoor effect in the quantized model (see the bottom curves of top subfigures in Figure 5). To overcome this issue, we adapt the projected gradient descent (PGD) [16, 17] optimization method to further constrain the parameter update in the fine-tuning stage of the model. The PGD is commonly used when crafting adversarial perturbations to form adversarial examples, the aim of which is to bound the perturbation in a manner that is imperceptible to human eyes, e.g., for images, or to stealthily maintain the semantics of the sample. The  $l_1$ -norm,  $l_2$ -norm and  $l_\infty$ -norm are widely used bounds.

We thus leverage the PGD to constrain the applied perturbations on the parameters with  $\epsilon_1$  difference in  $l_\infty$  norm space near  $\tilde{\Theta}_{bd}$  to ensure that  $\tilde{\Theta}_{rm}$  change in each update operation is relatively small. We denote this projection operator as  $P_{l_\infty}(AM(\Theta_{bd}), \epsilon_1)$ , where the maximum perturbation given a weight parameter is upperbounded by  $\epsilon_1$ . In a similar manner, the projection operator for constraining a scale factor  $S$  is defined as  $P_{l_\infty}(S_{bd}, \epsilon_2)$ , where the maximum perturbation given  $S$  is upperbounded by  $\epsilon_2$ .

**Constraining Weights.** Under the ideal situation of Equation 4, the absolute value of the fractional part of the affine mapping parameter  $AM(\Theta_{bd})$  of the backdoor model is close to 0. At this time,

as long as the affine mapping parameter  $AM(\Theta_{rm})$  of the fine-tuned model is constrained within the range of  $(AM(\Theta_{bd}) - 0.5, AM(\Theta_{bd}) + 0.5)$ , it can be ensured that the affine mapping parameters of the fine-tuning model after the rounding operation, that is, the quantized parameters  $\tilde{\Theta}_{rm}$  of the fine-tuned model, are the same as the quantization parameters  $\tilde{\Theta}_{bd}$  of the backdoored model. Thus, we set  $\epsilon_1$  to 0.5 and let  $AM(\Theta_{rm}) \in (AM(\Theta_{bd}) - 0.5, AM(\Theta_{bd}) + 0.5)$ , where 0.5 is the ideal setting for  $\epsilon_1$ , through the projection operator  $P_{l_\infty}(AM(\Theta_{bd}), 0.5)$  to achieve  $\text{Round}(AM(\Theta_{rm})) = \tilde{\Theta}_{bd}$ .

**Constraining Scale Factor.** Furthermore, the quantization constant scale factor  $S$  plays a decisive role in parameter quantization, in particular, during the float-32 emulation process. Although we restrict its update in Equation 4, it is far from sufficient and will still cause small changes in scale. However, even small changes will cause affine mapping values of the model parameters to produce large fluctuations in a float-32 format, so we set  $\epsilon_2$  to 0 to force the fine-tuned model  $M_{rm}$  to be consistent with the *scale* of each layer of the backdoored model  $M_{bd}$  using the projection operator  $P_{l_\infty}(S_{bd}, 0)$ .

In summary, the objective loss function  $L_{rm}$  is formulated as follows:

$$L_{rm} = L_3 + \lambda L_4 \quad (8)$$

s.t.  $P_{l_\infty}(AM(\Theta_{bd}), \epsilon_1 = 0.5), P_{l_\infty}(S_{bd}, \epsilon_2 = 0)$ ,

where  $L_3$  and  $L_4$  are given by Equation 6 and Equation 7. During this step via fine-tuning operation, we use the factor  $\lambda$  to regulate the importance of  $L_3$  and  $L_4$ . In our experiments, we simply set  $\lambda$  to 1.

The significance of constraining the perturbation amplitudes on weights and scale factor update is illustrated in Figure 5. Only when we employ the PGD with  $\epsilon_1 = 0.5$  and  $\epsilon_2 = 0$ , can the backdoor effect (quantized by the ASR) of  $\tilde{M}_{rm}$  retain stably while the backdoor effect is removed from  $M_{bd}$ . In other cases, the ASR of  $\tilde{M}_{rm}$  will decrease during the backdoor-unlearning process of  $M_{rm}$ .

## 5 EXPERIMENTAL VALIDATION

We first describe the experimental setup, including three popular model architectures and three datasets. We then introduce two key metrics, i.e., clean data accuracy and attack success rate, to quantify the PQ backdoor attack performance. Last, we present and analyze extensive experimental results, affirming the strength and practicality of PQ backdoor.

### 5.1 Experimental Setup

The PQ backdoor attack is implemented and tested using TensorFlow 2.5 framework. The Python version is 3.8.10. Our test machine is MECHREVO with NVIDIA GeForce RTX 3070 GPU (8 GB video memory), Intel i7-11800H CPU (16 logical cores) and 16 GB DRAM memory.

**5.1.1 Datasets.** We employed widely-used datasets, MNIST, CIFAR10 and GTSRB, for image classification tasks.

**MNIST/CIFAR10/GTSRB:** MNIST is a dataset of handwritten digits of 10 classes provided by different people [29]. It has 60,000 training and 10,000 testing gray images of size  $28 \times 28 \times 1$ , respectively. CIFAR10 [28] is a natural color image dataset for object

**Table 3: Clean model results as a baseline reference.**

Task	Model	Unquantized Model CDA	Quantized Model CDA
MNIST	VGG16	99.69%	99.68%
	ResNet18	99.72%	99.71%
	ResNet50	99.71%	99.71%
CIFAR10	VGG16	91.79%	91.85%
	ResNet18	93.44%	93.39%
	ResNet50	93.58%	93.58%
GTSRB	VGG16	98.68%	98.67%
	ResNet18	98.84%	98.83%
	ResNet50	99.15%	99.13%

recognition. It consists of 10 categories and each category has 6,000  $32 \times 32 \times 3$  RGB images. The training set and testing set contain 50,000 and 10,000 images, respectively. GTSRB [47] is a dataset for German Traffic Sign Recognition. There are 43 types of traffic signs. In the data preprocessing stage, all traffic signs are cut out from the image according to the bounding box coordinates and aligned uniformly into  $32 \times 32 \times 3$  RGB image. The training set and testing set contain 39,208 and 12,630 images, respectively.

We set a  $6 \times 6$  pixel patch in the right-bottom corner of the image to zero, that is, a white square is used as a trigger shown in Figure 3. We then alter labels of poisoned samples to a targeted label to facilitate the implementation of the PQ backdoor. We note that the datasets and trigger we used are used in the evaluation of previous backdoor defenses [6, 11, 31] including Neural Cleanse [52] and STRIP [15]. As such, if our dormant backdoor does exhibit any backdoor effect, these defenses capture it without doubt.

**5.1.2 Model Architecture.** As for the network architecture under attack, we consider three popular DL models suitable for recognition tasks: ResNet18, ResNet50 [21], and VGG16 [46]. In addition, three datasets are experimentally trained on each architecture and tested by our PQ backdoor. The results of these diverse network architectures and datasets are used to validate the generality of our attack.

For all tasks, we use the ADAM optimizer to train 100 epochs under the PQ training process, with a batch size of 32. The learning rate is at  $5 \times 10^{-4}$  when backdooring the full-precision model in the first step of PQ backdoor, and the learning rate is a bit smaller, being  $10^{-5}$  in the second step of our PQ backdoor.

### 5.2 Performance Metrics

To evaluate a backdoor, we use two widely used metrics: clean data accuracy (CDA) and attack success rate (ASR).

- **CDA** is the proportion of clean test samples with no trigger that are correctly predicted to their true labels.
- **ASR** is the proportion of test samples with a trigger that are predicted to attacker-targeted labels.

For the PQ backdoor attack, both CDA and ASR of  $M_{rm}$  should be comparable to that of a clean full-precision model counterpart. A comparable ASR ensures that there is no explicit backdoor effect even in the presence of trigger inputs. However, for the backdoored TFLite model  $\tilde{M}_{rm}$ , the ASR should be as high as possible, while the CDA should be comparable to that of a clean TFLite model counterpart.



**Table 4: PQ backdoored model results.**

Task	Model	Unquantized Model CDA	Unquantized Model ASR (before BR <sup>1</sup> ; after BR)	Quantized Model CDA	Quantized Model ASR
MNIST	VGG16	99.27%	100.00%; 1.04%	99.55%	99.26%
	ResNet18	99.41%	100.00%; 0.24%	99.65%	100.00%
	ResNet50	99.50%	100.00%; 0.22%	99.68%	99.96%
CIFAR10	VGG16	92.39%	99.78%; 0.81%	92.08%	99.35%
	ResNet18	93.93%	99.81%; 0.63%	93.47%	99.71%
	ResNet50	94.23%	99.88%; 0.50%	93.80%	99.78%
GTSRB	VGG16	98.65%	99.78%; 0.41%	98.85%	98.79%
	ResNet18	98.67%	99.88%; 0.25%	98.68%	99.84%
	ResNet50	98.65%	99.81%; 0.27%	99.11%	99.52%

<sup>1</sup> Backdoor Removal is abbreviated to BR.

### 5.3 Evaluation Results

To serve as a baseline reference, we have trained a clean full-precision model  $M_{cl}$  for each task per model architecture. The performance results are summarized in Table 3. Accordingly, each clean quantized model  $\tilde{M}_{cl} \leftarrow \text{quantize}(M_{cl})$  is obtained, and their performance is also evaluated. To specify, their CDAs are almost the same.

**5.3.1 Full Precision Model Behavior.** As shown in Table 4, the full-precision model  $M_{rm}$  (derived from  $M_{bd}$  by removing the backdoor effect) always has a similar CDA with its clean counterpart  $M_{cl}$ . This means that by examining the CDA of the returned full-precision model  $M_{rm}$  using clean validation samples, the user cannot perceive any malicious behavior.

As for the ASR of  $M_{rm}$ , it is always close to 0. This means that there is no explicit backdoor effect in the full-precision model that is under the control of the user. So any backdoor inspection on  $M_{rm}$  will fail, and would then be validated later. Note that the small but non-zero ASR (e.g., 0.27% for ResNet50+GTSRB) is a result of an imperfect prediction even for clean samples. In other words, a clean model cannot achieve 100% accuracy for clean inputs, and thus there are a few cases where clean inputs from class A are misclassified into class B that may be the targeted label. Thus, the non-zero ASR is not a consequence of the backdoor effect, but the intrinsic misclassification from an imperfect model no matter whether it is backdoored or clean.

**5.3.2 Quantized Model Behavior.** We now evaluate the performance of the quantized model  $\tilde{M}_{rm}$  that is converted from  $M_{rm}$ , which has no backdoor effect.

As for the CDA, it is clear that it is similar to the full-precision model. This has two implications. The first is that checking the CDA of  $\tilde{M}_{rm}$  cannot reveal any adversarial behavior. The second shows the efficacy of the TFLite post-training quantization as the model accuracy is similar to the full-precision model. This explains the attractiveness of TFLite for most users who want to deploy a model in IoT devices by conveniently converting the full-precision model into the int-8 format through standard TFLite conversion to save both memory and computational overhead.

As for the ASR,  $\tilde{M}_{rm}$  preserves high effectiveness with ASR in all cases close to 100%. As a comparison, this ASR is almost the same as the ASR of a backdoored full-precision model  $M_{bd}$  in the first step of the PQ backdoor attack. This means the second step of the

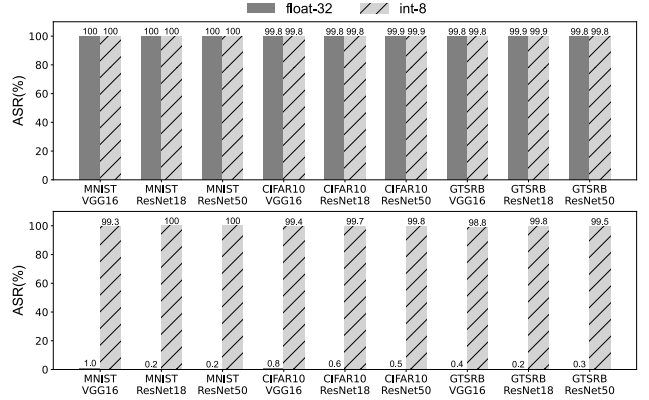


**Figure 6: (Top) The backdoor effect of the backdoored full-precision model will trivially propagate to its quantized model, as they share almost the same attack success rate (ASR). (Bottom) The backdoor effect of the quantized model remains to be high even though its full-precision model exhibits no explicitly backdoor behavior.**

PQ backdoor attack successfully preserves the backdoor effect for the quantized model while remove the effect from  $M_{rm}$ .

In summary, with nine backdoored models, we have confirmed the effectiveness of the PQ backdoor attack. A full-precision model exhibits no backdoor effect initially, but this effect can be activated once the standard TFLite post-training quantization operation is applied, as visualized and compared in Figure 6 (bottom) in Appendix. In this case, the quantized model exhibits a highly effective backdoor effect.

## 6 EVALUATION AND COMPARISON

Great efforts have been made to mitigate backdoor attacks recently [6, 15, 31, 48, 52, 55]. Here, we consider four defenses (or detection) including Neural Cleanse [52], STRIP [15], ABS [31], and the most recent MNTD [55] for evaluating the PQ backdoor attacks. Note that in cases where the full-precision model has a backdoor effect, any defense should be able to *robustly* capture it. This is because the backdoor attack is under the threat model of these defenses. More specifically, they can identify input-agnostic backdoor attacks where a small trigger is employed. The STRIP, ABS, and MNTD are insensitive to trigger size but Neural Cleanse is, and therefore we only choose a small trigger in our experiments in Section 5 so as not to violate each of the threat models. To facilitate the detection, we intentionally choose a white-square static trigger that is the easiest to be detected by all defenses rather than complicated triggers.

However, we identified that performance of ABS and MNTD were fairly non-robust (especially the MNTD), both of which fail to detect the backdoor post quantization but they should do. Therefore, the results of Neural Cleanse and STRIP are elaborated in great detail below. The results of ABS and MNTD are deferred to Appendix A.

### 6.1 Neural Cleanse

Neural Cleanse [52] builds upon the intuition that, given a backdoored model, merely a significantly small perturbation is needed

**Table 5: Backdoor detection performance of Neural Cleanse.**

Task	Model	Anomaly Index		
		$M_{bd}$	$M_{rm}$	$\tilde{M}_{rm}$
MNIST	VGG16	4.6	1.66	2.72
	ResNet18	<b>0.87</b>	0.90	<b>0.92</b>
	ResNet50	<b>20.7</b>	<b>56.9</b>	<b>0.91</b>
CIFAR10	VGG16	3.47	1.07	3.21
	ResNet18	3.94	1.16	3.11
	ResNet50	<b>1.08</b>	0.71	<b>0.91</b>
GTSRB	VGG16	3.23	1.13	<b>1.01</b>
	ResNet18	3.21	1.73	3.25
	ResNet50	<b>1.24</b>	1.42	<b>1.09</b>

Note: Anomaly index with **bold** font means that the model backdoor behavior is falsely judged. The anomaly index with **red** font exhibits an extreme abnormal behavior, which 10x deviates from other indices. In these two cases, the Neural Cleanse labels (0,8,4,3) classes and (8, 4) classes are attacker targeted classes for  $M_{bd}$  and  $M_{rm}$ , respectively. The target class is '0', so that the identified target label is completely erroneous for  $M_{rm}$ —the reverse-engineered trigger is also incorrect as shown in Figure 7. For all these backdoor detection cases except for ResNet50+MNIST, due to instability of Neural Cleanse [20, 51], the reverse-engineered triggers by Neural Cleanse also fail to capture the real trigger characteristics, as visualized in Figure 7.

to apply to any input sample in order to cause misclassification into the attacker-targeted (infected) label in comparison to the one that requires any uninfected labels. There are three general steps in Neural Cleanse process. First, given a label, the user employs an optimization scheme to find the minimal perturbation that is the potential trigger required to change *any* input of other labels into this chosen label. Second, a user repeats the first step for all labels as the chosen label, which produces  $N$  potential triggers given  $N$  classes needed to be classified by the model—the complexity of Neural Cleanse is thus related to  $N$ . Third, the user measures the size of each trigger by the number of pixels each trigger candidate has, i.e., how many pixels the trigger replaces, which is quantized by the  $l_1$ -norm. The smallest perturbation is regarded as the trigger, resembling the real trigger if its  $l_1$ -norm deviates significantly from other perturbations, which is determined via an outlier detection algorithm. Such a deviation is measured by a so-called anomaly index. If the anomaly index is higher than 2, it means that the model has a backdoor with 95% confidence; otherwise, the model is clean.

Backdoor detection performance of the Neural Cleanse against PQ backdoor is detailed in Table 5.<sup>7</sup> We can see the anomaly index of  $M_{rm}$  models is smaller than 2 when the Neural Cleanse stays stable. Therefore, the Neural Cleanse recognizes them as clean models. As a comparison, we have applied the Neural Cleanse on the backdoored full-precision models  $M_{bd}$ , and we can see that it correctly detects the backdoor in most cases as their anomaly indices are beyond the threshold of 2, in particular, for VGG16 and ResNet18 models. However, the Neural Cleanse, in some cases, is unstable when identifying backdoors given varying trigger size, shape, or pattern, which presents false alarms or true rejections [20]. Our evaluations also show a true rejection due to such instability when a larger model is used, (i.e., the ResNet50), where the Neural Cleanse fails

<sup>7</sup>Source code is from <https://github.com/bolunwang/backdoor>.

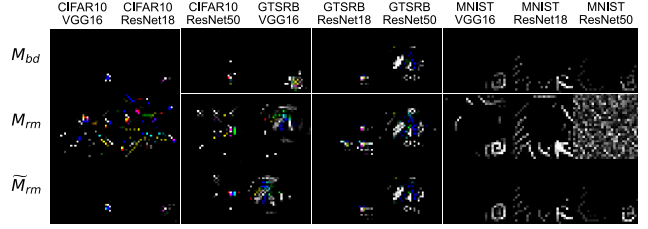


**Figure 7: Reverse-engineered triggers by Neural Cleanse. The target label is the '0' class in all cases. The real trigger is a  $6 \times 6$  white square at the right-bottom corner of an image shown in Figure 3.**

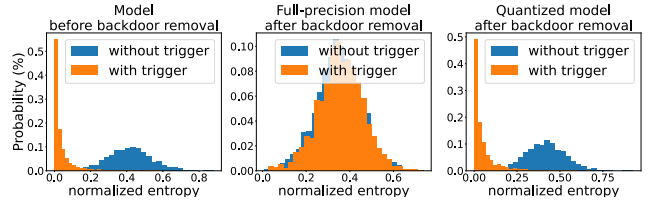


**Figure 8: Entropy distribution of the STRIP defense. (Left) the full-precision model  $M_{bd}$  is inspected. (Middle) the full-precision model  $M_{rm}$  after applying backdoor removal is inspected. (Right) the quantized model  $\tilde{M}_{rm}$  from  $M_{rm}$  is inspected. Model architecture is ResNet50 and the dataset CIFAR10 is used.**

to detect the backdoor for the backdoored full-precision model  $M_{bd}$  and the quantized model  $\tilde{M}_{rm}$ .

Figure 7 further visualizes the reverse-engineered triggers. Given the backdoored full-precision model  $M_{bd}$ , as shown in Figure 7 (top), the identified triggers are close to the real ones for VGG16 and ResNet18 models, but are uncorrelated to the real ones for the larger ResNet50 model trained on GTSRB. This further explains the failure backdoor detection for the ResNet50 model. As for the backdoor removed full-precision model  $M_{rm}$  as shown in Figure 7 (middle), under expectation the identified triggers are usually random.

## 6.2 STRIP

STRIP [15] turns the trigger input-agnostic strength into a weakness to detect whether a given input is a trigger or clean. The process is as follows. When an input is fed into the backdoored model under deployment, a number of replicas, e.g.,  $N = 20$ , of this input are created and each replica is injected with strong perturbations. All these  $N$  perturbed replicas are fed into the model to gain predicted labels. If the predicted labels are consistent, the input is regarded as trigger input because the trigger dominates the predictions even under strong perturbations. The consistency is quantized with entropy. A low entropy (randomness) of an input means that it is a trigger input; on the other hand, high entropy (randomness) indicates a clean input.

Figure 8 (left) shows the entropy distribution, given trigger inputs and clean inputs, when they are fed into the backdoored full-precision model  $M_{bd}$ <sup>8</sup>. Here, the model architecture is ResNet50

<sup>8</sup>Source code is from <https://github.com/garrisonsys/STRIP>.

and the CIFAR10 task is trained. Rest architecture and dataset combinations have also been evaluated, but their visualization results are omitted as they exhibit the same tendency to avoid redundancy. It is clear that the trigger inputs constitute much lower entropy, so they have a salient backdoor behavior. After the backdoor removal, when  $M_{\text{rm}}$  that the user will receive is inspected, it is impossible to distinguish trigger inputs from clean inputs. Because their entropy distribution greatly overlaps, all with high values, as shown in Figure 8 (middle),  $M_{\text{rm}}$  successfully evades the backdoor detection.

### 6.3 Inspecting Quantized Models

This is to further show that the backdoor effect of the quantized model is preserved where conventional backdoor detection methods can ordinarily capture them. Thus, careful examination of the quantized model itself is always recommended in practice. That is, one should not rely on the intuition that the security of the full-precision model will *correctly* propagate to the quantized model, despite the fact that this normally holds true.

Backdoor detection performance of Neural Cleanse against the quantized model  $\tilde{M}_{\text{rm}}$  is summarized in Table 5. As we can see, the backdoor is detected since the anomaly index is always higher than 2 for MNIST+VGG16, CIFAR10+ResNet50, GTSRB+VGG16 and GTSRB+ResNet50. For the rest, Neural Cleanse fails to detect them again due to its usability. Figure 7 (bottom) visualizes the reverse-engineered triggers in this case. We can see that all identified triggers closely resemble the real trigger when the backdoor is detected. As for those failed detections, the reverse-engineered trigger sometimes are still close to the real ones. This again indicates the unstability of the Neural Cleanse in a sense that some carefully tuning detection hyper-parameters is required, contingent on the dataset, model, even trigger shape, size, and pattern [20, 51]. The entropy distribution of trigger inputs and clean inputs given the STRIP inspection against the quantized model  $\tilde{M}_{\text{rm}}$  is shown in Figure 8 (right). As the backdoor effect is salient in  $\tilde{M}_{\text{rm}}$ , the two distributions are clearly distinct.

### 6.4 Attack Comparison

At a high level, a concurrent compression backdoor attack [51] recently proposed differs from our PQ backdoor in *two* major aspects. **Generality.** Tian *et al.* [51] have attacked the PyTorch Mobile framework, which is still in its beta stage and thus not as broad or versatile as the product-ready TFLite. Tian *et al.* do not show any attack feasibility on TFLite. In fact, as we detailed in Section 7.1, intuitive attacks on TFLite are difficult to execute and their attack methodology cannot stably apply to TFLite. In contrast to this concurrent work [51], our attack methodology is more generic. We have successfully applied our PQ backdoor against PyTorch Mobile. In the PyTorch Mobile framework, the int-8 quantization range is [-128, +127], and there are two types of quantization back-ends: fbgemm for x86 architecture and qnnpack for ARM-based mobile device. With VGG16+CIFAR10 and the same square trigger used previously, we have tested our PQ backdoor on both backends, where the results are summarized in Table 8.

We have further evaluated two detection methods of Neural Cleanse and STRIP. As can be seen from results of Neural Cleanse (i.e., Table 9 and Figure 10) as well as STRIP (i.e., Figure 11), both

defenses are unable to identify the backdoor (here we test on input-agnostic backdoor attack) of the front-end full-precision model but are still effective against the quantized backdoored models. We conclude that all results of attacks and defenses on PyTorch Mobile are aligned with those on TFLite.

**Efficiency.** Our attack implementation differs greatly from the work [51], and we achieve a much higher and more stable attack performance. In fact, Tian *et al.* carry out an intuitive attack strategy as detailed in Section 7.1, which potentially explains their unstable attack performance. As shown in the paper [51], the ASR is merely about  $42.3\% \pm 46.6\%$  (46.6% is the standard deviation) given a ResNet18 trained over CIFAR10. This ASR is still only  $80\% \pm 37.2\%$  when further optimization strategies are applied, e.g., only few layers (layers from the fourth group of basic blocks of the ResNet18) are attacked instead of all model layers. Overall, its attack performance appears to be sensitive to both the model and dataset. In contrast, our attack performance through a distinct efficient implementation is extremely stable, achieving close to 100% ASR for all cases against TFLite as well as PyTorch Mobile as shown in Table 8. In addition, we have easily attacked ResNet50 that is a deeper network (see Section 4), while the deepest network is ResNet18 in [51]. Moreover, opposed to our PQ backdoor that is *insensitive* to the calibration dataset (see Section 7.2), the attack of Tian *et al.*'s work [51] is sensitive, especially when a different distribution calibration dataset is applied, resulting in a notable drop on the ASR.

## 7 DISCUSSION

In this section, we comprehensively discuss the PQ backdoor.

### 7.1 Intuitive PQ Backdoor

Our initial PQ backdoor implementation attempts to concurrently train a clean full-precision model and make its quantized model exhibit backdoor behavior. In this context, the objective loss function is as follows:

$$L = \sum_{x \in D} (\text{loss}(M(x), y) + \text{loss}(\tilde{M}(x), y)) + \sum_{x_t \in D_c} (\text{loss}(M(x_t), y) + \sum_{x_t \in D_t} \text{loss}(\tilde{M}(x_t), y_t)). \quad (9)$$

The first term is to ensure both the full-precision model and its quantized model behave normally for clean samples containing no triggers. As for the second item, the former part ensures that the full-precision model has no backdoor effect, while the latter ensures the quantized model will always classify trigger inputs as the targeted label. Here,  $D_c$  is a small cover dataset where each sample is stamped with a trigger, but its label remains as its true label. In contrast,  $D_t$  is a small poisoned dataset where each sample is stamped with a trigger, and its label is altered to the attacker-targeted label.

However, this implementation has not succeeded in our experiments. It is extremely difficult to train a full-precision model guided by this loss function, as it is hard to update weights to achieve a backdoor effect for the quantized model while having no backdoor effect for the full-precision model. The training curve is shown in Figure 9. As we can see from the CDA (left), the int-8 model degrades after 50 epochs, and then severely fluctuates. As for the

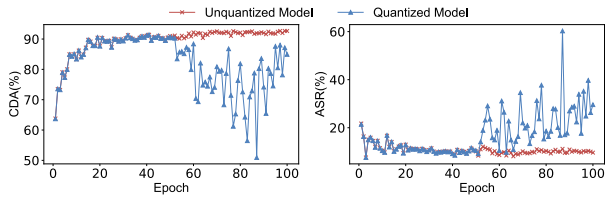


Figure 9: Training curves when using an intuitive objective loss function in Equation 9 to direct PQ backdoor optimization. The ResNet18 is used to train CIFAR10.

Table 6: Quantized model performance across calibration datasets.

	CIFAR10 (same)	CIFAR100 (similar)	GTSRB (different)
CDA of $\tilde{M}_{rm}$	92.69%	91.39%	90.89%
ASR of $\tilde{M}_{rm}$	99.99%	99.70%	100%

\*For each case, 100 images are randomly selected (the default number as per TFLite guide) to constitute a calibration dataset.

ASR, though the int-8 model sees improvements after 50 epochs, it is hard to achieve a high performance. In addition, it also exhibits severe fluctuations. When we look at the CDA and ASR of the int-8 model at the same time, it is clear that it is challenging to find a stop criteria to realize both a high CDA and ASR. Therefore, it is extremely challenging for the PQ backdoor to converge, which results in the failure of this intuitive PQ backdoor implementation.

## 7.2 Insensitivity to Calibration Datasets

We now investigate the PQ backdoor sensitivity to calibration datasets. In practice, when a user downloads a full-precision model, the model provider may not provide a calibration dataset associated with the task. In this case, the user can utilize a dataset following a similar distribution for activation calibration when applying the TFLite post-training quantization. Table 6 shows the quantized model’s CDA and ASR when varied calibration datasets are leveraged. Here, the model architecture is ResNet18 trained over CIFAR10. Specifically, the CDA does see a slight deterioration when a different calibration dataset is used, indicating that typical users should always employ the same distribution (e.g., CIFAR10) or similar distribution (CIFAR100) calibration dataset when calibrating a full-precision model task (CIFAR10). Nonetheless, for the PQ backdoor attack, we concern the ASR. We can see from the table that the ASR is insensitive to calibration datasets.

## 7.3 Complicated Backdoor Variants

In previous experiments, we use a common source-agnostic/input-agnostic backdoor with a simple trigger, which can be detected if an user inspects the quantized model. However, it should be noted that backdoor inspection of quantized model *does not fully guarantee a backdoor-free quantized model*, although it can reduce the risks.

Regarding attack-defense arms race, adaptive attacks could be carefully designed to bypass devised defenses [44] even under their threat model assumptions. In addition, each defense usually has its own specific assumptions, and therefore, once the attacker uses an attack strategy beyond the defense threat model, the defense can be trivially bypassed. For example, a large trigger size can easily defeat

Table 7: The results of the PQ backdoor model based on DQR

Task	Model	Quantized Model	
		CDA	ASR
CIFAR10	VGG16	92.01%	99.40%
	ResNet18	93.53%	99.71%
	ResNet50	93.86%	99.81%

Table 8: PQ backdoor against PyTorch Mobile (int-8).

	CDA	ASR
$M_{rm}$	92.58%	0.7%
$\tilde{M}_{rm}$ (fbgemm for x86 backend)	92.59%	99.51%
$\tilde{M}_{rm}$ (qnnpack for ARM backend)	92.63%	99.52%

Neural Cleanse [52], DeepInspect [6], and Februss [11]. Implementing the source-specific backdoor attack can trivially evade source-agnostic backdoor focused defenses, such as Neural Cleanse [52], STRIP [14, 15], and ABS [31], which we have experimentally demonstrated and detailed in Appendix B by extensive evaluations. *In summary, complicated backdoor variants can be easily incorporated with PQ backdoor to enable the quantized model to trivially evade state-of-the-art defenses (Neural Cleanse, STRIP, ABS, and MNTD we tested).*

## 7.4 Other Quantization Methods and Tasks

TFLite provides several post-quantization methods, and we have mainly focused on the full-integer quantization (FIQ) method in previous experiments because it has the best memory efficiency, and most importantly, it fits best for IoT devices using microcontrollers. Here, we show that other configurations, in particular, dynamic range quantization (DRQ) method (the model size reduced by 4 $\times$ ) if chosen by the user can also be vulnerable to the presented PQ backdoor. According to the TFLite’s optimization framework, FIQ and DRQ have the same quantization process for weights. The main difference is that the FIQ activations are quantified with the assistance of a calibration set, while the DRQ activations are dynamically quantified during the inference process without the calibration set. Our attack implementation is insensitive to how the activation values are quantified. Thus, it is possible to activate the backdoors of the quantized model converted by the DRQ method when the full-precision model is attacked through the FIQ method. In particular, its attack success rate against DRQ is comparable to that of the quantization model by using FIQ, which is validated by the experimental results detailed in Table 7. Here, the CIFAR10 is used, and the full-precision model is originally used to attack FIQ but quantized through the DRQ method.

Although this work uses image classification for extensive validations, we expect that other tasks such as image segmentation, object detection, as well as tasks from audio and textual domains are also vulnerable to the quantization backdoor attack. We leave these as future works. In addition, it is expected that models with a larger number of parameters are more vulnerable to a concealed dormant quantization backdoor.

**Table 9: Backdoor detection performance of Neural Cleanse for PyTorch Mobile.**

	Anomaly Index
$M_{rm}$	1.24
$\tilde{M}_{rm}$ (fbgemm for x86 backend)	2.57
$\tilde{M}_{rm}$ (qnnpack for ARM backend)	3.32

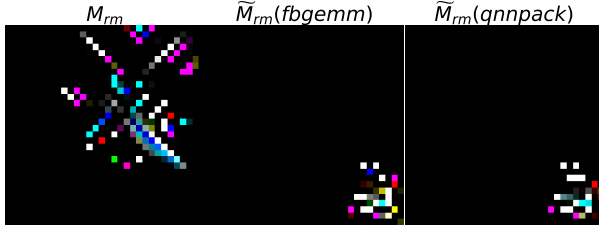


**Figure 10: Reverse-engineered trigger of Neural Cleanse for PyTorch Mobile PQ backdoored model. The reverse-engineered trigger of the front-end full-precision model  $M_{rm}$  is completely inaccurate.**

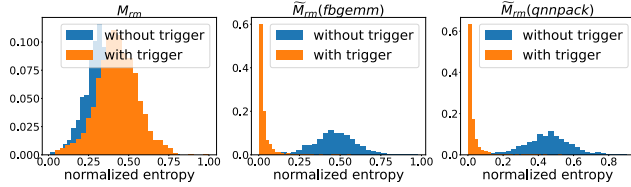


**Figure 11: Entropy distribution of the STRIP defense. The PyTorch Mobile framework is attacked by the PQ backdoor.**

## 8 CONCLUSION

By exploiting the inevitable truncation errors when converting a high-precision value to its low-precision counterpart, we reveal that current two most popular post quantization frameworks include the product-ready TFLite are vulnerable to a new quantization backdoor attack, threatening their secure usability. We have demonstrated that this attack can be practically realized through the formulated implementations. Building upon TFLite and PyTorch Mobile commercial frameworks, extensive experiments affirm that the full-precision model successfully evades state-of-the-art backdoor inspections while its quantized model still achieves non-degraded effect with a close to 100% ASR and a CDA comparable to its clean model counterpart. In addition, we have experimentally shown that different post-quantization methods (i.e., full integer and dynamic range quantizations provided by TFLite framework) are vulnerable to the presented PQ backdoor. Furthermore, the complicated backdoor variants can be trivially incorporated with the PQ backdoor to render not only front-end full-precision model but also quantized model inspections to be further challenging.

## REFERENCES

- [1] Martin Abadi, Paul Barham, Jianmin Chen, Zhifeng Chen, Andy Davis, Jeffrey Dean, Matthieu Devin, Sanjay Ghemawat, Geoffrey Irving, Michael Isard, et al. 2016. Tensorflow: A system for large-scale machine learning. In *12th USENIX symposium on operating systems design and implementation (OSDI)*, 265–283.
- [2] Yossi Adi, Carsten Baum, Moustapha Cisse, Benny Pinkas, and Joseph Keshet. 2018. Turning your weakness into a strength: Watermarking deep neural networks by backdooring. In *27th USENIX Security Symposium*, 1615–1631. <https://www.usenix.org/conference/usenixsecurity18/presentation/adi>
- [3] Renzo Andri, Lukas Cavigelli, Davide Rossi, and Luca Benini. 2017. YodaNN: An architecture for ultralow power binary-weight CNN acceleration. *IEEE*

- Transactions on Computer-Aided Design of Integrated Circuits and Systems* 37, 1 (2017), 48–60.
- [4] Eugene Bagdasaryan, Andreas Veit, Yiqing Hua, Deborah Estrin, and Vitaly Shmatikov. 2020. How to backdoor federated learning. In *International Conference on Artificial Intelligence and Statistics*. PMLR, 2938–2948.
- [5] Adrian Bulat and Georgios Tzimiropoulos. 2019. XNOR-Net++: Improved binary neural networks. In *British Machine Vision Conference (BMVC)*. <https://arxiv.org/abs/1909.13863>
- [6] Huili Chen, Cheng Fu, Jishen Zhao, and Farinaz Koushanfar. 2019. DeepInspect: A Black-box Trojan Detection and Mitigation Framework for Deep Neural Networks. In *Proceedings of the 28th International Joint Conference on Artificial Intelligence*. AAAI Press, 4658–4664.
- [7] Xinyun Chen, Chang Liu, Bo Li, Kimberly Lu, and Dawn Song. 2017. Targeted backdoor attacks on deep learning systems using data poisoning. *arXiv preprint arXiv:1712.05526* (2017).
- [8] Francesco Conti, Pasquale Davide Schiavone, and Luca Benini. 2018. XNOR neural engine: A hardware accelerator IP for 21.6-fj/op binary neural network inference. *IEEE Transactions on Computer-Aided Design of Integrated Circuits and Systems* 37, 11 (2018), 2940–2951.
- [9] Robert David, Jared Duke, Advait Jain, Vijay Janapa Reddi, Nat Jeffries, Jian Li, Nick Kreeger, Ian Nappier, Megha Natraj, Shlomi Regev, et al. 2020. TensorFlow Lite Micro: Embedded Machine Learning on TinyML Systems. *arXiv preprint arXiv:2010.08678* (2020).
- [10] Tim Davis and T.J. Alumbaugh. July 2021. TensorFlow Lite: ML for mobile and IoT devices (TF Dev Summit '20). <https://www.youtube.com/watch?v=27Zx-4GOQAs>
- [11] Bao Gia Doan, Ehsan Abbasnejad, and Damith C Ranasinghe. 2020. Februus: Input purification defense against Trojan attacks on deep neural network systems. In *Annual Computer Security Applications Conference*, 897–912.
- [12] Facebook. July 2021. Pytorch Mobile: End-to-end workflow from Training to Deployment for iOS and Android mobile devices. <https://pytorch.org/mobile/home/>
- [13] Yansong Gao, Bao Gia Doan, Zhi Zhang, Siqi Ma, Anmin Fu, Surya Nepal, and Hyounghick Kim. 2020. Backdoor attacks and countermeasures on deep learning: a comprehensive review. *arXiv preprint arXiv:2007.10760* (2020).
- [14] Yansong Gao, Yeonjae Kim, Bao Gia Doan, Zhi Zhang, Gongxuan Zhang, Surya Nepal, Damith Ranasinghe, and Hyounghick Kim. 2021, DOI: 10.1109/TDSC.2021.3055844. Design and Evaluation of a Multi-Domain Trojan-Detection Method on Deep Neural Networks. *IEEE Transactions on Dependable and Secure Computing* (2021, DOI: 10.1109/TDSC.2021.3055844).
- [15] Yansong Gao, Change Xu, Derui Wang, Shipping Chen, Damith C Ranasinghe, and Surya Nepal. 2019. STRIP: A defence against trojan attacks on deep neural networks. In *Proceedings of the 35th Annual Computer Security Applications Conference*, 113–125.
- [16] Siddhant Garg, Adarsh Kumar, Vibhor Goel, and Yingyu Liang. 2020. Can adversarial weight perturbations inject neural backdoors. In *Proceedings of the 29th ACM International Conference on Information & Knowledge Management*, 2029–2032.
- [17] Ian J Goodfellow, Jonathon Shlens, and Christian Szegedy. 2014. Explaining and harnessing adversarial examples. *arXiv preprint arXiv:1412.6572* (2014).
- [18] Google. July 2021. Deploy machine learning models on mobile and IoT devices. <https://www.tensorflow.org/lite>
- [19] Tianyu Gu, Brendan Dolan-Gavitt, and Siddharth Garg. 2017. Badnets: Identifying vulnerabilities in the machine learning model supply chain. *arXiv preprint arXiv:1708.06733* (2017).
- [20] Wenbo Guo, Lun Wang, Xinyu Xing, Min Du, and Dawn Song. 2019. TABOR: A Highly Accurate Approach to Inspecting and Restoring Trojan Backdoors in AI Systems. *arXiv preprint arXiv:1908.01763* (2019).
- [21] Kaiming He, Xiangyu Zhang, Shaoqing Ren, and Jian Sun. 2016. Deep residual learning for image recognition. In *Proceedings of the IEEE Conference on Computer Vision and Pattern Recognition*, 770–778.
- [22] Itay Hubara, Matthieu Courbariaux, Daniel Soudry, Ran El-Yaniv, and Yoshua Bengio. 2016. Binarized neural networks. *Advances in Neural Information Processing Systems* 29 (2016), 4107–4115.
- [23] Itay Hubara, Yury Nahshan, Yair Hanani, Ron Banner, and Daniel Soudry. 2021. Accurate Post Training Quantization With Small Calibration Sets. In *International Conference on Machine Learning*. PMLR, 4466–4475.
- [24] Benoit Jacob, Skirmantas Kligys, Bo Chen, Menglong Zhu, Matthew Tang, Andrew Howard, Hartwig Adam, and Dmitry Kalenichenko. 2018. Quantization and training of neural networks for efficient integer-arithmetic-only inference. In *Proceedings of the IEEE Conference on Computer Vision and Pattern Recognition*, 2704–2713.
- [25] Yujie Ji, Xinyang Zhang, Shouling Ji, Xiapu Luo, and Ting Wang. 2018. Model-reuse attacks on deep learning systems. In *Proceedings of the 2018 ACM SIGSAC Conference on Computer and Communications Security*. ACM, 349–363.
- [26] Hengrui Jia, Christopher A Choquette-Choo, Varun Chandrasekaran, and Nicolas Papernot. 2021. Entangled watermarks as a defense against model extraction. In *30th USENIX Security Symposium*.

- [27] NG Karthikeyan. 2018. Machine Learning Projects for Mobile Applications: Build Android and IOS Applications Using TensorFlow Lite and Core ML. Packt Publishing Limited.
- [28] Alex Krizhevsky, Geoffrey Hinton, et al. 2009. Learning multiple layers of features from tiny images. Technical Report. Citeseer. <http://citeseerx.ist.psu.edu/viewdoc/download?doi=10.1.1.222.9220&rep=rep1&type=pdf>
- [29] Yann LeCun, Léon Bottou, Yoshua Bengio, and Patrick Haffner. 1998. Gradient-based learning applied to document recognition. Proc. IEEE 86, 11 (1998), 2278–2324.
- [30] Yu Li, Min Li, Bo Luo, Ye Tian, and Qiang Xu. 2020. DeepDyve: Dynamic Verification for Deep Neural Networks. In Proceedings of the 2020 ACM SIGSAC Conference on Computer and Communications Security. 101–112.
- [31] Yingqi Liu, Wen-Chuan Lee, Guanhong Tao, Shiqing Ma, Yousra Aafer, and Xiangyu Zhang. 2019. ABS: Scanning Neural Networks for Backdoors by Artificial Brain Stimulation. In Proceedings of the 2018 ACM SIGSAC Conference on Computer and Communications Security.
- [32] Yingqi Liu, Shiqing Ma, Yousra Aafer, Wen-Chuan Lee, Juan Zhai, Weihang Wang, and Xiangyu Zhang. 2018. Trojaning attack on neural networks. In Network and Distributed System Security Symposium (NDSS).
- [33] Zechun Liu, Zhiqiang Shen, Marios Savvides, and Kwang-Ting Cheng. 2020. ReactNet: Towards precise binary neural network with generalized activation functions. In European Conference on Computer Vision. Springer, 143–159.
- [34] The Machine. July 2021. Why TinyML is a giant opportunity. <https://venturebeat.com/2020/01/11/why-tinyml-is-a-giant-opportunity/>
- [35] Brais Martinez, Jing Yang, Adrian Bulat, and Georgios Tzimiropoulos. 2020. Training binary neural networks with real-to-binary convolutions. In International Conference on Learning Representations (ICLR). <https://arxiv.org/abs/2003.11535>
- [36] Markus Nagel, Rana Ali Amjad, Mart Van Baalen, Christos Louizos, and Tijmen Blankevoort. 2020. Up or down? adaptive rounding for post-training quantization. In International Conference on Machine Learning. PMLR, 7197–7206.
- [37] Haotong Qin, Ruihao Gong, Xianglong Liu, Xiao Bai, Jingkuan Song, and Nicu Sebe. 2020. Binary neural networks: A survey. Pattern Recognition (2020), 107281.
- [38] Huming Qiu, Hua Ma, Zhi Zhang, Yifeng Zheng, Anmin Fu, Pan Zhou, Yansong Gao, Derek Abbott, and Said F Al-Sarawi. 2021. RBNN: Memory-Efficient Reconfigurable Deep Binary Neural Network with IP Protection for Internet of Things. arXiv preprint arXiv:2105.03822 (2021).
- [39] Erwin Quiring and Konrad Rieck. 2020. Backdooring and poisoning neural networks with image-scaling attacks. In 2020 IEEE Security and Privacy Workshops (SPW). IEEE, 41–47.
- [40] Mohammad Rastegari, Vicente Ordonez, Joseph Redmon, and Ali Farhadi. 2016. XNOR-net: Imagenet classification using binary convolutional neural networks. In European Conference on Computer Vision. Springer, 525–542.
- [41] Aniruddha Saha, Akshayvarun Subramanya, and Hamed Pirsiavash. 2020. Hidden trigger backdoor attacks. In Proceedings of the AAAI Conference on Artificial Intelligence, Vol. 34. 11957–11965.
- [42] Ali Shafahi, W Ronny Huang, Mahyar Najibi, Octavian Suci, Christoph Studer, Tudor Dumitras, and Tom Goldstein. 2018. Poison frogs! targeted clean-label poisoning attacks on neural networks. arXiv preprint arXiv:1804.00792 (2018).
- [43] Shawn Shan, Emily Wenger, Bolun Wang, Bo Li, Haitao Zheng, and Ben Y Zhao. 2020. Gotta Catch ‘Em All: Using Honey pots to Catch Adversarial Attacks on Neural Networks. In Proceedings of the ACM SIGSAC Conference on Computer and Communications Security. 67–83.
- [44] Reza Shokri et al. 2020. Bypassing backdoor detection algorithms in deep learning. In 2020 IEEE European Symposium on Security and Privacy (EuroS&P). IEEE, 175–183.
- [45] Li Shuangfeng. 2020. Tensorflow Lite: On-device machine learning framework. Journal of Computer Research and Development 57, 9 (2020), 1839.
- [46] Karen Simonyan and Andrew Zisserman. 2014. Very deep convolutional networks for large-scale image recognition. arXiv preprint arXiv:1409.1556 (2014).
- [47] Johannes Stalkamp, Marc Schlipf, Jan Salmen, and Christian Igel. 2012. Man vs. computer: Benchmarking machine learning algorithms for traffic sign recognition. Neural Networks 32 (2012), 323–332.
- [48] Di Tang, XiaoFeng Wang, Haixu Tang, and Kehuan Zhang. 2021. Demon in the Variant: Statistical Analysis of DNNs for Robust Backdoor Contamination Detection. In 30th USENIX Security Symposium.
- [49] Tensorflow Team. July 2021. Post-training quantization. [https://www.tensorflow.org/lite/performance/post\\_training\\_quantization](https://www.tensorflow.org/lite/performance/post_training_quantization)
- [50] Tensorflow-Lite. July 2021. Representative Dataset. [https://tensorflow.google.cn/lite/api\\_docs/python/tf/lite/RepresentativeDataset](https://tensorflow.google.cn/lite/api_docs/python/tf/lite/RepresentativeDataset)
- [51] Yulong Tian, Fnu Suya, Fengyuan Xu, and David Evans. 2021. Stealthy Backdoors as Compression Artifacts. arXiv preprint arXiv:2104.15129 (2021).
- [52] Bolun Wang, Yuanshun Yao, Shawn Shan, Huiying Li, Bimal Viswanath, Haitao Zheng, and Ben Y Zhao. 2019. Neural Cleanse: Identifying and mitigating backdoor attacks in neural networks. In 2019 IEEE Symposium on Security and Privacy (SP). IEEE, 707–723.
- [53] Pete Warden and Daniel Situnayake. 2019. TinyML: Machine learning with Tensorflow Lite on arduino and ultra-low-power microcontrollers. O’Reilly Media.
- [54] Qixue Xiao, Yufei Chen, Chao Shen, Yu Chen, and Kang Li. 2019. Seeing is not believing: Camouflage attacks on image scaling algorithms. In 28th USENIX Security Symposium. 443–460.
- [55] Xiaojun Xu, Qi Wang, Huichen Li, Nikita Borisov, Carl A Gunter, and Bo Li. 2021. Detecting AI trojans using meta neural analysis. In IEEE Symposium on Security and Privacy (SP).
- [56] Yuanshun Yao, Huiying Li, Haitao Zheng, and Ben Y Zhao. 2019. Latent backdoor attacks on deep neural networks. In Proceedings of the 2019 ACM SIGSAC Conference on Computer and Communications Security. 2041–2055.
- [57] Yichi Zhang, Junhao Pan, Xinheng Liu, Hongzheng Chen, Deming Chen, and Zhiru Zhang. 2021. FracBNN: Accurate and FPGA-Efficient Binary Neural Networks with Fractional Activations. In The 2021 ACM/SIGDA International Symposium on Field-Programmable Gate Arrays. 171–182.

## APPENDIX

### A NON-ROBUSTNESS OF ABS AND MNTD

In our experiments, we observe that the ABS and MNTD are fairly non-robust, especially the MNTD. Specifically, they are unable to detect the backdoor of the quantized models though they claim to do so. Because the input-agnostic backdoor attack with the small square trigger we use is one of the easiest cases that all backdoor defenses should be able to catch if they are relatively robust. Below we detail the findings in our experiments based on their original source code.

#### A.1 ABS

The ABS [31] iteratively scans every inner neuron by changing its value while retaining all remaining neurons unchanged and then observes the impact of the changed neuron on the output activations change, which is used to identify potential compromised neurons by the backdoor. A threshold based on REASR (attack success rate of reverse-engineered trojan triggers) score is used to decide whether a model under test is backdoored or not. If a model’s REASR score is higher than the threshold, the model is regarded as backdoored; otherwise it is benign.

We follow the threshold score of 0.88 used in the original source code for evaluation. Figure 12 displays Max REASR scores of benign models and the backdoored models. A model is believed to have a backdoor when its max REASR is greater than the threshold, i.e., 0.88. From left to right in Figure 12 are the results from MNIST, CIAFR10, and GTSRB, with VGG16 as the model architecture. Specifically, 20 benign models  $M_{cl}$  and 20 backdoored models  $M_{rm}$  are trained respectively on each of the three tasks, and then the REASR score of each model is measured by the ABS. By injecting 1.5% poisonous data, the ASR of the backdoored model before quantization is lower than 1%, while the ASR of the backdoored model after quantization is always higher than 99% and its CDA is comparable to its counterpart clean model. As we can clearly see from Figure 12, the ABS regards full-precision models  $M_{rm}$  as benign. The max REASR of  $M_{cl}$  and  $M_{rm}$  are close to each other in different tasks.

We further quantize the full-precision model  $M_{rm}$  into its int-8 model  $\tilde{M}_{rm}$  and evaluate the ABS detection effectiveness. In this case, if the ABS is robust, it should be able to detect  $\tilde{M}_{rm}$  as backdoored. However, as detailed in Figure 12, the results are similar to that of  $M_{rm}$ . Unlike the Neural Cleanse and STRIP that can detect the backdoor activated in  $\tilde{M}_{rm}$ , the ABS fails to detect the backdoor even after quantization.

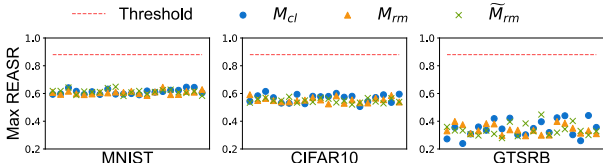


Figure 12: The max REASR of  $M_{cl}$ ,  $M_{rm}$ , and  $\tilde{M}_{rm}$  measured by the ABS. The model is backdoored if its max REASR score is above the threshold. The model architecture is VGG16.

#### A.2 MNTD

Given a task/dataset, the MNTD [55] trains many shadow models including backdoored and benign ones. Then it feeds samples into these shadow models to collect outputs (i.e., logits). Finally, the MNTD uses the concatenated outputs along with their labels (backdoored or benign) as input vectors to train a meta-classifier, which is used to determine whether a model-under-test trained with the same dataset is backdoored or benign.

We re-implement the MNTD solely based on its released source code [55].<sup>9</sup> The dataset we used follows the work [55], i.e., CIFAR10. The performance of MNTD is fairly non-robust based on our extensive reproduction evaluations when we test it against conventional backdoored models, in particular,  $M_{bd}$  in our case. Nonetheless, we apply it to test  $M_{rm}$  and  $\tilde{M}_{rm}$ . Note that the MNTD uses AUC as a main metric, which assumes that a number of backdoored models and benign models trained over the same task/dataset are under test. This is somehow unrealistic because the model-under-test given the same task in practice is usually the only one model (i.e., benign or backdoored).

As the original work does not specify how to evaluate a single model, we instead use the following steps to do so. Given a single target model, the meta-classifier outputs a score for that model to measure its maliciousness. However, this score is not constrained by the sigmoid activation function, which indicates that the score of the target model does not represent the probability that the model has a backdoor. Thus, a meta-classifier uses a threshold to aid in decision making, and it selects the median score of all shadow models in this meta-classifier training set as the threshold. A target model (i.e., model under test) is considered to be backdoored when its score is greater than the threshold; otherwise it is benign. Notably, a total of five meta-classifiers with different initialization settings are trained by MNTD to jointly decide whether a backdoor exists in the target model. But the MNTD does not explicitly clarify how the decision is jointly made. Here, we adopt the common technique of majority voting, that is, if the majority of five meta-classifiers believes the existence of a backdoor, then the model under test is considered to be backdoored.

We train 5 meta-classifiers (using shadow benign models  $M_{cl}$  and shadow backdoored models  $M_{bd}$ ) on the CIFAR10, exactly the same to the source code, to detect a test model set that contains 20 positive samples (benign model) and 20 negative samples (backdoored model). The model structure used for the test set is VGG16. A PQ backdoor attack is used to inject a backdoor into the models as a negative sample (i.e.,  $M_{rm}$  and  $\tilde{M}_{rm}$ , respectively), where all test models are trained until convergence. We report the threshold and median test model scores on each meta-classifier. Following this method described in the MNTD, it is found that the test model scores were generally higher than the threshold of the meta-classifier, which means that the meta-classifier would consider all the test models to have backdoors even if it is benign. When we adopt the majority voting to evaluate the accuracy and average AUC of the meta-classifiers on the test set, the results are summarized in Table 10. We can see that the MNTD appears to do random guessing. More

<sup>9</sup>The source code is from <https://github.com/AI-secure/Meta-Neural-Trojan-Detection>.

**Table 10: Thresholds of each meta-classifier and its evaluation results for PQ backdoor attacks. Five meta-classifiers in total.**

meta-classifier No.	Threshold	$M_{rm}$			$\tilde{M}_{rm}$		
		Median of test model scores	Average AUC	Accuracy	Median of test model scores	Average AUC	Accuracy
1 <sup>th</sup>	-2.74	4.87	49.60%	50.00%	4.75	46.50%	50.00%
2 <sup>th</sup>	-0.57	2.51			2.54		
3 <sup>th</sup>	0.13	13.27			13.37		
4 <sup>th</sup>	-2.62	6.77			6.56		
5 <sup>th</sup>	-4.29	8.51			8.44		

**Table 11: The performance of the PQ backdoored model incorporating source-specific attacks and the detection results of various defenses. The model is ResNet18 trained on CIFAR10 dataset.**

	$M_{cl}$	$M_{bd}$	$M_{rm}$	$\tilde{M}_{rm}$
CDA	93.44%	93.37%	93.56%	93.26%
ASR	N/A	97.50%	0.60%	97.50%
Anomaly index (Neural Cleanse)	1.32	0.97	1.73	0.96
Max REASR (ABS)	53.41%	56.74%	50.36%	53.69%
Average AUC (MNTD)	50.17%	53.87%	51.95%	53.08%

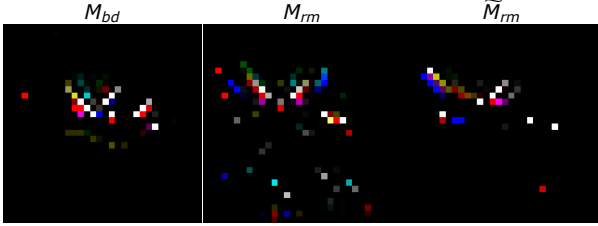


**Figure 13: Reverse-engineered trigger of Neural Cleanse for source-specific PQ backdoor attack.**

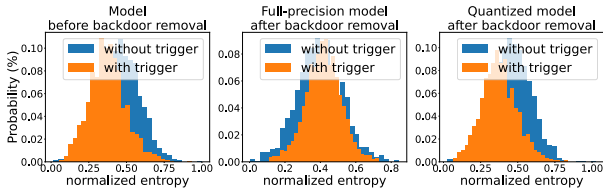


**Figure 14: Entropy distribution of the STRIP defense. The source-specific PQ backdoor attack is evaluated.**

specifically, similar to ABS, it also fails to detect the backdoor in  $\tilde{M}_{rm}$  that it is ought to do so.

## B PQ BACKDOOR INCORPORATED WITH SOURCE-SPECIFIC BACKDOOR VARIANTS

In all previous experiments, we intentionally use a simple small trigger and an input-agnostic backdoor attack. This setting, under the threat model of defenses such as Neural Cleanse and STRIP, is tailored for defenses that can readily capture the backdoor behavior if the full-precision model does exhibit.

It is not non-trivial to perform a stealthier PQ backdoor by incorporating a backdoor variant technique to evade defenses even when they are used to inspect quantized models. Specifically, we consider a source-specific PQ backdoor and confirm that it can bypass the evaluated defenses, i.e., Neural Cleanse, STRIP, ABS and MNTD. In this setting, the model is ResNet18 and the dataset is CIFAR10. The trigger is 6x6 square located at the bottom right corner. The source class is class 1 and the target class is 0, and all other classes are non-source classes. This means the backdoor effect is only triggered when the trigger is stamped with a sample from the source class 1. The non-source class sample with a trigger does not have the backdoor effect. The attack performance of the source-specific PQ backdoor is detailed in Table 11 (second row). It is clear that the PQ backdoor is still effective.

The results of four defenses are summarized as follows.

- **Neural Cleanse.** As detailed in Table 11 (third row), we can see the anomaly index of backdoored model regardless of full-precision  $M_{rm}$  or quantized  $\tilde{M}_{rm}$  is lower than 2.0, which means the backdoor is undetected. Figure 13 shows reverse-engineered triggers, which are erroneous throughout backdoored models.
- **ABS.** As detailed in Table 11 (fourth row), the Max REASR of backdoored models are close to clean models (both lower than the threshold of 0.88), which cannot be distinguished by the ABS.
- **MNTD.** As detailed in Table 11 (last row), the AUC is close to 50% in all cases, which implies that the MNTD determines the backdoored model by random guess.
- **STRIP.** As shown in Figure 14, the entropy distributions of the trigger inputs and normal inputs given the backdoored models heavily overlap, which indicates that the STRIP fails.

In summary, the PQ backdoor using advanced backdoor variants trivially bypasses the model inspection against both the front-end full precision model and the quantized model.